PRAMANA
— journal of
physics

Vol. 85, No. 5
November 2015
pp. 1033–1055

Solitons in a hard-core bosonic system: Gross–Pitaevskii type and beyond

RADHA BALAKRISHNAN[1,*] and INDUBALA I SATIJA[2]

[1]The Institute of Mathematical Sciences, C.I.T. Campus, Chennai 600 113, India
[2]School of Physics, Astronomy and Computational Sciences, George Mason University, Fairfax VA 22030, USA
*Corresponding author. E-mail: radha@imsc.res.in

DOI: 10.1007/s12043-015-1113-6; ***e*Publication:** 20 October 2015

Abstract. We present a unified formulation to investigate solitons for all background densities in the Bose–Einstein condensate of a system of hard-core bosons with nearest-neighbour attractive interactions, using an extended Bose–Hubbard lattice model. We derive in detail the characteristics of the solitons supported in the continuum version, for the various cases possible. In general, two species of solitons appear: A nonpersistent (NP) type that fully delocalizes at its maximum speed and a persistent (P) type that survives even at its maximum speed. When the background condensate density is nonzero, both species coexist, the soliton is associated with a constant intrinsic frequency, and its maximum speed is the speed of sound. In contrast, when the background condensate density is zero, the system has neither a fixed frequency, nor a speed of sound. Here, the maximum soliton speed depends on the frequency, which can be tuned to lead to a cross-over between the NP-type and the P-type at a certain critical frequency, determined by the energy parameters of the system. We provide a single functional form for the soliton profile, from which diverse characteristics for various background densities can be obtained. Using mapping to spin systems enables us to characterize, in a unified fashion, the corresponding class of magnetic solitons in Heisenberg spin chains with different types of anisotropy.

Keywords. Solitons; Bose–Einstein condensate; hard-core bosons; Bose–Hubbard model.

PACS Nos 05.45.Yv; 03.75.Kk; 42.50.Lc

1. Introduction

Experimental demonstration [1–6] of solitary waves/solitons [7] in Bose–Einstein condensates (BEC) [8,9] is one of the hallmarks of the quantum coherence inherent in ultracold atomic systems. As predicted theoretically from the Gross–Pitaevskii equation (GPE) [9], which describes weakly interacting bosons in the mean-field approximation, a condensate of Rb atoms with repulsive interactions was found to support dark solitary waves (density depressions) [1], while a Li condensate [2] with attractive interactions

supported bright solitary waves (density elevations) [10]. Intrinsically nonlinear, BEC systems continue to remain an active area to explore the presence of nonlinear localized modes. In view of the fact that the GPE also describes nonlinear optical systems, these studies are relevant beyond the BEC context.

In our earlier work [11–13], we have investigated the propagation of solitonic excitations in a system of hard-core bosons (HCB), which describes strongly repulsive bosons. Mapping an extended Bose–Hubbard model [14,15] for hard-core bosons on a lattice (with nearest-neighbour (*nn*) hopping energy t and *nn* interaction energy V) to a spin model, we used spin-coherent states [16] to obtain the condensate density for the HCB system as $\rho^{\mathrm{s}} = \rho(1-\rho)$, where ρ is the bosonic (particle) density for the HCB system. We derived the continuum evolution equation for the condensate wave function, which we called the HGPE, 'H' standing for HCB. The only model-dependent effective energy parameter that appears in the HGPE is $E_e = (t - V)/t$. (It is convenient to express all energies in units of t, which sets the energy scale in the problem.)

In the case $E_e > 0$, we analysed unidirectional solitary wave excitations in the HGPE when the background density ρ_0 contains both particles and holes. For a hard-core system, this implies $0 < \rho_0 < 1$. We refer to this as the 'fractional-filling' case. This corresponds to a nonzero condensate density ρ_0^{s} in the background. Under these conditions, the system was shown to possess an intrinsic speed of sound and an intrinsic frequency parameter. These are fixed in the sense that they depend on the given background density and the system parameters. This frequency can be shown to be just the frequency associated with the phase of the homogeneous condensate in the background.

At half-filling, the density ρ can exhibit both bright and dark solitons which are mirror images of each other. Further, both are nonpersistent (NP) solitons that flatten out and delocalize at their maximum speed, which is the speed of sound in the system. Intriguingly, for half-filling, the behaviour of solitons in the condensate density ρ^{s} in this strongly repulsive system can be shown to be [13] very similar to that of the GP soliton in a weakly repulsive system, because it is dark, and delocalizes at sonic speed.

Away from half-filling, we found two distinct species of solitons that coexist in the HCB system. For $0 < \rho_0 < \frac{1}{2}$ (respectively, $\frac{1}{2} < \rho_0 < 1$), one is a NP-type dark (resp., bright) soliton in the density, that delocalizes completely at the speed of sound, while the other is a novel persistent P-type bright (resp., dark) soliton that survives as a localized entity, even at its maximum speed. In addition, the P-type soliton transforms into a train of solitons at supersonic speeds, quite unlike a GP soliton. The corresponding condensate density soliton of the NP type is always dark, while that of the P type not only survives at the speed of sound, but also becomes completely bright at this speed [11,12]. This brightness is quite unexpected in a very strongly repulsive system like the HCB. Preliminary results on the collision properties of these solitary waves [17] show that they emerge unscathed, suggesting that they could be strict solitons. Additionally, in a recent study [18], we have also shown that both the above species of solitary waves found in the continuum analytically, remain stable on the discrete lattice under time evolution, and also survive quantum fluctuations, for experimentally accessible time-scales.

A natural question that arises is whether the HCB system can support solitary wave excitations for $E_e > 0$, when the background density has only particles or only holes, i.e., when $\rho_0 = 1$ or when $\rho_0 = 0$. We shall refer to both these limiting values as the 'integer filling' case, in which the condensate density in the background vanishes, i.e., $\rho_0^{\mathrm{s}} = 0$.

In contrast to the case of fractional filling, in the integer filling case there is neither an intrinsic speed of sound to limit the soliton speed, nor a fixed intrinsic frequency. Another interesting aspect worth exploring is the existence of solitons when $E_e \leq 0$, for both fractional and integer filling.

In this paper we present new results addressing these issues, in the framework of a unified formulation that leads to a single functional form for density solitons, which is valid for both fractional-filling and integer-filling background densities, when $E_e > 0$ as well as $E_e \leq 0$. Using this form, we deduce diverse characteristics of solitons in various cases possible. In the case of fractional filling [11,12], the soliton is characterized only by its speed. We find that, for integer filling, the soliton is characterized both by its speed and by its independently tunable frequency parameter ω. Interestingly, the maximum soliton speed is seen to depend on ω, leading to two competing energy scales, $E_\omega = \hbar\omega/t$ and the effective energy E_e.

When $E_e > 0$ and we have integer filling, both NP and P solitons appear, but they do not coexist. Depending upon the relative strengths of E_ω and E_e, the system supports either a P soliton that persists at its (frequency-dependent) maximum speed, or an NP soliton which delocalizes at this speed. Thus the frequency can be tuned to lead to a cross-over between the NP soliton and the P soliton at a certain critical frequency that is determined by E_e.

When $E_e \leq 0$, we show that while only NP solitons are supported for integer fillings, no soliton solutions exist for fractional-filling backgrounds.

A general interesting feature of HCB solitons for the integer-filling background (for all E_e) is that, unlike the fractional-filling case where the maximum soliton speed is limited by the speed of sound, high-speed solitons are possible here, because the maximum soliton speed is controlled by the tunable frequency.

Finally, using the mapping of HCB to spins, the single functional form we obtain for the density soliton also enables us to classify, in a unified fashion, the characteristics of magnetic solitons in the isotropic Heisenberg spin chain as well as in the easy-plane and easy-axis anisotropic spin chains.

2. The extended Bose–Hubbard model

2.1 *The model Hamiltonian*

As is well known, by loading ultracold bosonic atoms onto an optical lattice [19] created using standing waves of laser light, it has become possible to realize various models of condensed matter systems in the laboratory. More important, it is also possible to create lattices of different dimensions, as well as tune the value of the parameters in the model, experimentally. This motivates us to consider the following Hamiltonian for the extended Bose–Hubbard (BH) lattice model [14] in d dimensions:

$$H = -\sum_{\langle j,l\rangle} \left[t(b_j^\dagger b_l + \text{h.c.}) + V n_j n_l \right] + \sum_j \left[U n_j (n_j - 1) + 2t n_j \right]. \qquad (1)$$

Here, j is a site index, $\langle j, l\rangle$ denotes nearest-neighbour sites, $b_j^\dagger$ and b_j are the usual boson creation and annihilation operators satisfying the commutation relations $[b_i, b_j^\dagger] = \delta_{ij}$ and

$[b_i, n_j] = b_i \delta_{ij}$, where n_j is the number operator at site j. As already mentioned, t is the *nn* hopping energy parameter and V is the *nn* interaction, while U denotes the on-site repulsive energy. The on-site term $2tn_j$ has been added so as to obtain the correct kinetic energy term in the continuum version of the many-body bosonic Hamiltonian, which will also enable direct comparison with the usual form of the GPE.

While several aspects of the model given by eq. (1) such as quantum phase transitions, phase diagrams, etc. have been studied [14], our interest here is to investigate whether this model can support nonlinear dynamical excitations like solitons.

2.2 *BEC evolution for weakly repulsive normal bosons and GPE: Order parameter evolution using bosonic coherent states*

Before proceeding to our study of BEC in a strongly repulsive boson system described by hard-core bosons, it is instructive to study the connection between GPE describing weakly repulsive bosons and the usual BH model for normal bosons, i.e., eq. (1) without the *nn* interaction term.

The GPE can be derived (see, for instance [12]) by starting with the many-body Hamiltonian for an interacting boson system described in terms of boson field operators $\Psi(r, t)$ and a two-body interaction $\bar{V}(r - r')$. Invoking the concept of a broken gauge symmetry, the BEC order parameter (also called the condensate wave function) is conventionally defined as the expectation value of the boson annihilation operator, $\psi = \langle \Psi \rangle$ which becomes nonzero below the condensation temperature. For dilute, weakly interacting bosons, the boson interactions occur via low-energy, s-wave, two-body collisions. It can be shown that for such interactions $\bar{V}(r - r')$ can be replaced by a contact pseudopotential $g\delta(r - r')$, with $g \equiv 4\pi\hbar^2\bar{a}/m$, where $\bar{a}$ is the s-wave scattering length. Writing the equation of motion for the operator Ψ, we can derive the equation of motion for the order parameter ψ by using the mean-field approximation, to give the following GPE:

$$i\hbar\psi_\tau + \frac{\hbar^2}{2m}\nabla^2\psi - g|\psi|^2\psi = 0. \tag{2}$$

Here, ψ_τ denotes the derivative of ψ with respect to time τ. As is well known, $g < 0\ (>0)$ corresponds to attractive (repulsive) interactions.

Now let us consider the usual BH lattice model (as opposed to the extended BH model of eq. (1)) which contains only the on-site finite repulsion term U and no *nn* interaction term V. As already mentioned, the order parameter of a BEC is defined as the expectation value of the boson annihilation operator. It has been argued [20] that the Glauber (or bosonic) coherent state representation may be appropriate for computing this expectation value, because it is well known that coherent states are most useful in the context of many-body systems which display quantum effects on macroscopic scales as in a BEC.

Taking the expectation value in a boson coherent state of both sides of the Heisenberg equation of motion $i\hbar b_{j,\tau} = [b_j, H]$ using the Hamiltonian for the usual BH lattice model, we obtain the evolution equation for the order parameter $\langle b_j \rangle$. A short calculation shows that its continuum version is identical in form to the GPE given in eq. (2), on identifying the hopping parameter t with $\hbar^2/(ma^2)$ where a is the lattice spacing, and U with $g \equiv 4\pi\hbar^2\bar{a}/m$. Note that since $U > 0$ for the BH model, eq. (2) obtained here describes the condensate dynamics for weak repulsive interaction between bosons.

It is to be noted that the use of boson coherent state expectation values leads to a mean-field description, so that for the GPE, the condensate density ρ^s is equal to the particle density ρ.

Although unidirectional soliton solutions of the GPE are well known, our analysis presented below differs from those discussed in the BEC soliton literature [9,10]. As we shall see, our systematic methodology for obtaining solitons in this weakly repulsive GPE will also be useful in arriving at a unified formulation for finding soliton solutions for BEC in the strongly repulsive system described by hard-core bosons, for various background densities.

It is well known that linear modes of the GPE can be found by analysing small-amplitude travelling wave solutions of eq. (2) to yield the Bogoliubov dispersion relation [9], which shows that the modes are sound waves with speed $c_g = (g\rho_0/m)^{1/2}$. In order to study solitons (in the x-direction), we first set $\psi = \sqrt{\rho(x,\tau)}\,\exp[i\phi(x,\tau)]$ in eq. (2), and separate its real and imaginary parts to obtain coupled equations for ρ and ϕ. We then seek travelling wave solutions of the form

$$\rho(x,\tau) = \rho_0 + f(z) \quad \text{and} \quad \phi(x,\tau) = \omega\tau + \phi(z), \tag{3}$$

where $z = (x - v\tau)$. Here, v is the speed of the travelling wave and ω is a frequency parameter. Using eq. (3) in the coupled equations for ρ and ϕ obtained from eq. (2), a lengthy but straightforward calculation yields

$$-v\rho_z + \frac{\hbar}{m}(\rho\phi_z)_z = 0 \tag{4}$$

and

$$-4\hbar\rho^2\omega + 4\hbar\rho^2 v\phi_z + \frac{\hbar^2}{m}\rho\rho_{zz} - \frac{\hbar^2}{2m}\rho_z^2 - \frac{2\hbar^2}{m}\rho^2\phi_z^2 - 4g\rho^3 = 0, \tag{5}$$

where the subscript z stands for the derivative with respect to z.

We are interested in soliton solutions with boundary conditions $\rho(z) \to \rho_0$ and the derivative $\phi_z \to 0$, as $|z| \to \infty$. Equation (4) can then be integrated easily to yield

$$\phi_z = \frac{mv(\rho - \rho_0)}{\hbar\rho}. \tag{6}$$

Substituting for ϕ_z from eq. (6) into eq. (5), multiplying by ρ_z/ρ^2 and collecting terms appropriately, the resulting equation can be integrated to yield

$$\frac{\hbar^2}{2m}\rho_z^2 = 2g\rho^3 - (2mv^2 - 4\hbar\omega)\rho^2 - \lambda_g\rho - 2mv^2\rho_0^2, \tag{7}$$

where λ_g is a constant of integration to be determined consistently. We have used the subscript g to indicate that the quantity concerned corresponds to the GPE case.

Note that the right-hand side of eq. (7) is a cubic polynomial in ρ. We are interested in finding localized solutions for $\rho(z)$, such that $\rho \to \rho_0$ and the slope $\rho_z \to 0$ asymptotically. With this requirement in mind, we write eq. (7) in the form

$$\frac{\hbar^2}{2m}\rho_z^2 = (\rho - \rho_0)^2\,(M_g\rho + N_g). \tag{8}$$

Then, equating the coefficients of like powers of ρ on the right-hand sides of eqs (7) and (8), we get (for $\rho_0 \neq 0$)

$$M_g = 2g, \quad N_g = -2mv^2, \quad \lambda_g = -2\rho_0[g\rho_0 + 2mv^2] \tag{9}$$

and

$$\omega = \omega_g = -g\rho_0/\hbar. \tag{10}$$

Thus, the frequency ω that appears in eq. (3) is a constant for the GP soliton. Looking for solutions of the form $\rho(z) = \rho_0 + f(z)$, and substituting for M_g and N_g in eq. (8), we get

$$\frac{\hbar}{2m}\frac{\mathrm{d}f}{\mathrm{d}z} = \pm f\left[\frac{fg}{m} + c_g^2\gamma_g^2\right], \tag{11}$$

where $c_g = \sqrt{g\rho_0/m}$ is the Bogoliubov speed of sound as already defined and $\gamma_g^2 = 1 - v^2/c_g^2$. Equation (11) can be integrated to give

$$f(z) = -\rho_0\,\gamma_g^2\,\mathrm{sech}^2(m\gamma_g c_g z/\hbar), \tag{12}$$

yielding the well-known GP dark soliton solution

$$\rho(z) = \rho_0\big[1 - \gamma_g^2\,\mathrm{sech}^2(m\gamma_g c_g z/\hbar)\big]. \tag{13}$$

This is a soliton that describes a depression in the background density ρ_0. Its profile flattens out as v tends to the speed of sound c_g. Thus, the GP dark soliton is of NP-type.

The phase of the soliton is obtained by substituting eq. (13) into eq. (6) and integrating it, to get $\phi(z) = -\tan^{-1}[(\gamma_g c_g/v)\tanh(m\gamma_g c_g z/\hbar)]$. This yields the phase jump across the soliton to be $\Delta\phi = -2\cos^{-1}(v/c_g)$.

It is important to note that while we looked for solutions for ρ and ϕ as in eq. (3) with two parameters v and ω, eq. (10) shows that, for the GP soliton, the frequency $\omega = \omega_g = -g\rho_0/\hbar$ is not a variable parameter, but is determined by the local repulsion energy g and the background condensate density ρ_0. Thus, the GP soliton has only a single variable parameter, its speed v, which cannot exceed the speed of sound. Further, an inspection of eq. (2) shows that ω_g has its origin in the purely time-dependent phase $\phi = \omega_g\tau$ associated with the background condensate density ρ_0, which is nonzero for the GP soliton. In other words, $\hbar\omega_g$ can be regarded as the energy of the background.

2.3 *Hard-core boson limit*

It is instructive to write the solution for f in terms of the BH model parameters by setting $\hbar = m = 1$ and $g = U$ (with U expressed in units of t):

$$f(z) = -\frac{c_g^2\gamma_g^2}{U[\cosh(2\gamma_g c_g z) + 1]}. \tag{14}$$

The HCB limit corresponds to $U \to \infty$. This implies $c_g^2 \to \infty$ and $\gamma_g \to 1$. Hence the GP soliton (13) flattens out and delocalizes in this limit.

Before concluding this section on GPE, in the interest of completeness we point out that solitons in the GPE for a BEC in a quasi-one-dimensional, cigar-shaped trap has been studied extensively [21–23]. Here, bosons are confined using a harmonic potential of

frequency ω_T, which is transverse to the axis along which the soliton propagates. Starting with the 3D-GPE given in eq. (2) and using an appropriate product wave function, it becomes possible to study both weak and strong interacting limits. For the former, one obtains a 1D-GPE with a renormalized coupling which depends on ω_T. Hence, its soliton solution can be easily written down using our preceding analysis.

The strongly interacting case [21,22] corresponds to the condition $\rho_0 g \gg \hbar\omega_T$, in our notation. On using Thomas–Fermi approximation for the transverse profile, the GPE (2) reduces to a 1D nonlinear Schrödinger equation with a quadratic nonlinearity. In [23] two possible soliton solutions have been found for this equation. While these strong coupling solutions are valid for large, finite g values, it is easy to verify that both solutions flatten out and delocalize in the hard-core boson limit $g \to \infty$. This is not surprising because in this extreme limit, normal boson commutation relations are not satisfied (as we shall see in the next section), thereby making the GPE given in (2) itself invalid in this limit. In the next section, we shall derive the appropriate order parameter evolution equation for a hard-core boson condensate.

3. BEC evolution for strongly repulsive bosons and HGPE: Order parameter evolution using spin-coherent states

We are now interested in studying the condensate of a strongly repulsive boson system, described by the hard-core boson limit $U \to \infty$ of the BH model.

3.1 *HCB system: Mapping to a spin-half Hamiltonian*

The limit $U \to \infty$ in the Hamiltonian (1) implies that two bosons cannot occupy the same site. This property can be incorporated (for all dimensions) by employing boson operators that anticommute at the same site but commute at different sites [15] . This leads to $b_j^2 = 0,\ n_j^2 = n_j,\ \{b_j,\ b_j^\dagger\} = 1,\ [b_j,\ b_l^\dagger] = (1 - 2n_j)\,\delta_{jl}$. Identifying $b_j = S_j^+$ (the spin-raising operator) and $n_j = \frac{1}{2} - S_j^z$ yields the spin-$\frac{1}{2}$ algebra, $[S_j^+,\ S_l^-] = 2S_j^z\,\delta_{jl}$. The extended Bose–Hubbard Hamiltonian (1) for HCB then maps to [15] the following quantum, spin-half, XXZ Heisenberg ferromagnetic (as $t > 0$) Hamiltonian in a magnetic field along the z-axis:

$$H_S = -\sum_{\langle j,l\rangle}\left[t(S_j^+ S_l^- + \text{h.c.}) + VS_j^z S_l^z\right] - d\sum_j (t - V)S_j^z. \tag{15}$$

3.2 *Order parameter evolution for the HCB system: HGPE*

The dynamics of the HCB system is given by the Heisenberg equation of motion,

$$i\hbar\dot{S}_j^+ = [S_j^+, H_S] = d(t - V)S_j^+ - tS_j^z\sum_l S_l^+ + VS_j^+\sum_l S_l^z, \tag{16}$$

where l runs over the nearest-neighbour sites of the site j. As the condensate order parameter is the expectation value of the boson operator b_j for the hard-core system, it is now given by $\langle S_j^+\rangle \equiv \eta_j$.

We use spin-coherent states [16] as the natural choice for computing the above expectation value, due to the inherent coherence in the condensed phase of the HCB system [11,12]. This is analogous to the use of boson coherent states for defining the order parameter of a weakly repulsive system of normal bosons, which leads to the GPE, as we have seen earlier.

The general spin-S coherent state at a lattice site l is defined by

$$|\tau_l\rangle = (1 + |\tau_l|^2)\exp(\tau_l S_l^-)|S\rangle, \tag{17}$$

where $S_l^- = S_l^x - iS_l^y$ is the spin-lowering operator, τ_l is a complex quantity and $S_l^z|S\rangle = S|S\rangle$. For N spins, we work with the direct product $|\tau\rangle = \Pi_l^N|\tau_l\rangle$. The states $|\tau_l\rangle$ are normalized, nonorthogonal and over-complete. It can be shown that the diagonal matrix elements of single spin operators in the spin-coherent representation are identical to the corresponding expressions for a classical spin [16]. For $S = \frac{1}{2}$, it can be shown that the condensate number density $\rho_j^{\rm s} = |\eta_j|^2$ and the particle number density $\rho_j = \langle n_j\rangle$ are related by [11,12]

$$\rho_j^{\rm s} = \rho_j(1 - \rho_j) = \rho_j\rho_j^{\rm h}, \tag{18}$$

where $\rho_j^{\rm h} = (1 - \rho_j)$ is the hole density. Hence both particles and holes play equally important roles in determining the condensate properties. Further, in contrast to the GPE case, $\rho^{\rm s} \neq \rho$. This implies the presence of depletion in the HCB system.

As explained in [11,12], taking the spin-coherent state expectation value of eq. (16) leads to the evolution equation for the order parameter $\eta_j = \langle S_j^+\rangle$ on the lattice. A continuum description of the discrete equations is useful when the order parameter is a smoothly varying function with a length scale greater than the lattice spacing a. Using appropriate Taylor expansions for the various quantities appearing in the lattice equations [11,12], we get

$$i\hbar\frac{\partial\eta}{\partial\tau} = -\frac{ta^2}{2}(1 - 2\rho)\nabla^2\eta - Va^2\eta\,\nabla^2\rho + 2d(t - V)\rho\eta, \tag{19}$$

where τ denotes time, as before. This is the HGPE (H representing HCB). Note that in eq. (19), the condensate wave function is given by

$$\begin{aligned}\eta(\mathbf{r},\tau) &= \sqrt{\rho^{\rm s}(\mathbf{r},\tau)}\exp[i\phi(\mathbf{r},\tau)]\\ &= \sqrt{\rho(\mathbf{r},\tau)(1 - \rho(\mathbf{r},\tau))}\,\exp[i\phi(\mathbf{r},\tau)],\end{aligned} \tag{20}$$

where we have used eq. (18). Substituting eq. (20) into eq. (19), coupled nonlinear evolution equations can be written down for the particle density ρ and the phase ϕ. From their solution, the condensate density $\rho^{\rm s} = \rho(1 - \rho)$ as well as the condensate wave function η can be found.

While our discussion so far is for d dimensions, our interest in this paper is to investigate solitons in the BEC of HCB, loaded appropriately on an effective one-dimensional lattice. We shall therefore set $d = 1$ in what follows, and look for unidirectional travelling wave solutions along the x-axis.

4. Some general features of the HGPE

Before presenting our analysis of soliton solutions of the HGPE, we point out some general features of the condensate parameter evolution of the HCB system as described by

eq. (19). These will be useful in understanding various characteristics of the soliton solutions we shall find for this system.

4.1 *GPE as a certain low-density approximation to HGPE*

From eq. (18), we note that in the low-density approximation, we can set $\rho^{\rm s} \approx \rho$. Using this in eq. (20), we have $\eta \to \psi = \sqrt{\rho}\,{\rm e}^{i\phi}$. In addition, if we also neglect nonlinear terms proportional to $\rho\nabla^2\eta$ and $\eta\nabla^2\rho$ in eq. (19), we get the GPE given in eq. (2), but with the identification $ta^2 = \hbar^2/m$, and with $2(t - V)$ as an effective local interaction between the (hard-core) bosons in the GPE limit. While the coupling constant g in eq. (2) (obtained from the usual BH model) is always positive, the coupling $2(t - V)$ arising as an approximation to the condensate dynamics of the extended BH model for HCB can be positive, negative or zero. However, as found earlier in the context of the GPE, the speed of sound will now be given by $[2(t - V)\rho_0/m]^{1/2}$, for the approximated HGPE under consideration. Hence there exists a speed of sound in this limit only when $(t - V) > 0$.

4.2 *Particle–hole symmetry*

In the HGPE (19), if we set $(1 - 2\rho) = (\rho^{\rm h} - \rho)$, so that $\rho = [1 + (\rho - \rho^{\rm h})]/2$, we get

$$i\hbar\,\frac{\partial\eta}{\partial\tau} = -\frac{ta^2}{2}(\rho^{\rm h} - \rho)\eta_{xx} - \frac{Va^2}{2}\,(\rho - \rho^{\rm h})_{xx}\eta + (t - V)(\rho - \rho^{\rm h})\eta + (t - V)\eta. \tag{21}$$

We may use the gauge transformation

$$\eta \to \eta{\rm e}^{-i(t-V)\tau/\hbar} \tag{22}$$

to remove the last term in eq. (21). This yields

$$i\hbar\,\frac{\partial\eta}{\partial\tau} = -\frac{ta^2}{2}(\rho^{\rm h} - \rho)\eta_{xx} - \frac{Va^2}{2}\,(\rho - \rho_h)_{xx}\eta + (t - V)(\rho - \rho^{\rm h})\eta. \tag{23}$$

We observe that interchanging the particle density ρ and the hole density $\rho^{\rm h}$ changes the overall sign of the right-hand side of this equation, and that η remains invariant under this interchange. This shows that if η is the wave function for the condensate of particles, η^* becomes the wave function for the condensate of holes. Thus, eq. (23) has a particle–hole symmetry that proves to be convenient for obtaining a unified formulation of the HCB condensate dynamics that we seek. Rewriting eq. (23) in terms of ρ alone, we have

$$i\hbar\,\frac{\partial\eta}{\partial\tau} = -\frac{ta^2}{2}(1 - 2\rho)\eta_{xx} - Va^2\rho_{xx}\eta + (t - V)(2\rho - 1)\eta. \tag{24}$$

4.3 *Fractional-filling and integer-filling background densities: Differences in physical characteristics*

One usually looks for solutions for the condensate that are asymptotically spatially homogeneous, i.e., $\rho \to \rho_0$ and $\eta \to [\rho_0(1 - \rho_0)]^{1/2}\,{\rm e}^{i\phi_{\pm\infty}}$. On substituting these asymptotic forms into eq. (24), we find that for fractional-filling backgrounds $0 < \rho_0 < 1$ (so that the

condensate background density is nonzero asymptotically), the phase must have a purely time-dependent term $\omega_{\rm F}\tau$ as well. Here the intrinsic frequency is given in terms of the system parameters by

$$\hbar\omega_{\rm F}/t = E_e(1-2\rho_0), \tag{25}$$

where $E_e = (t-V)/t$ is the dimensionless effective energy parameter, as already defined. (The subscript in $\omega_{\rm F}$ denotes fractional filling.) In contrast, for integer filling ($\rho_0 = 0$ or 1, implying a vanishing background condensate density), eq. (24) is identically satisfied asymptotically. Hence the frequency ω does not get determined, and remains a variable parameter.

The particle–hole symmetry of the intrinsic frequency is manifest in eq. (25). Regarding $\omega_{\rm F}$ as a function of ρ_0, we have

$$\omega_{\rm F}(\rho_0) = -\omega_{\rm F}(1-\rho_0) = -\omega_{\rm F}(\rho^{\rm h}). \tag{26}$$

Another feature that emerges is the following. Linear excitations of the HGPE analysed using small-amplitude solutions of eq. (19) yield the expression [11,12]

$$c \sim [2E_e\rho_0(1-\rho_0)]^{1/2} \tag{27}$$

for the speed of sound in the HCB condensate. This implies that while there are sound wave modes in a fractional-filling background when $E_e > 0$, they are absent in the integer-filling case. For $E_e \leq 0$, the HCB system does not support sound waves for any filling.

Consistent with the above observations, we shall indeed find that soliton solutions with fractional-filling and integer-filling background densities belong to two distinct classes, with only the former getting associated with a fixed frequency $\omega_{\rm F}$ as given by eq. (25) and a speed of sound as in eq. (27).

5. Soliton solutions for the HGPE

Setting $\eta = \rho(1-\rho)$ in eq. (24) and equating real and imaginary parts, we obtain the following coupled equations for ρ and ϕ:

$$\frac{\hbar\rho_\tau}{t} = -a^2[\rho(1-\rho)\phi_x]_x \tag{28}$$

and

$$\frac{\hbar\phi_\tau}{t} = E_e(1-2\rho) + \frac{a^2}{4}\Big[\frac{\rho_{xx}}{\rho(1-\rho)} - \frac{(1-2\rho)\rho_x^2}{2\rho^2(1-\rho)^2}\Big] - E_e a^2\rho_{xx} - \frac{a^2}{2}(1-2\rho)\phi_x^2. \tag{29}$$

5.1 *Exact nonlinear plane-wave solutions*

Although our interest is in finding soliton solutions which are localized in space, it is interesting to note that the coupled nonlinear PDEs (28) and (29) have exact plane-wave solutions. Taking $\rho(x,\tau) = \rho_0$, eq. (28) gives $\phi_{xx} = 0$. This leads to a plane-wave

solution $\phi(x,\tau) = -kx + \Omega\tau$. Using this in eq. (29), we get the exact dispersion relation for the plane waves, quadratic in k:

$$\hbar\Omega(k)/t = \hbar\omega_{\rm F}/t - \left(\frac{1}{2} - \rho_0\right) a^2 k^2, \tag{30}$$

where $\omega_{\rm F}$ is given by eq. (25). Thus, for $\rho_0 > \frac{1}{2}$, the plane-wave excitation is particle-like, whereas for $\rho_0 < \frac{1}{2}$ it is hole-like. When $\rho_0 = \frac{1}{2}$, $\Omega(k)$ vanishes, showing that the plane wave becomes static.

5.2 *Solitons for fractional- and integer-filling backgrounds: A unified formulation*

While the methodology that we shall use to find solitary wave solutions of the HGPE will be in close parallel to that of the GPE discussed in the last section, the HGPE will be seen to support both bright and dark solitons, in contrast to the GPE which has only dark solitons. This arises essentially due to a particle–hole symmetry in the HCB model.

Looking for unidirectional travelling waves of the typical form (3), eqs (28) and (29) become

$$v\rho_z = \left[\rho(1-\rho)\phi_z\right]_z \tag{31}$$

and

$$\begin{aligned}(E_\omega - v\phi_z)\,\rho_z \;=\; & E_e(1-2\rho)\rho_z + \frac{1}{8}\Big[\frac{\rho_z^2}{\rho(1-\rho)}\Big]_z \\ & -E_e\rho_{zz}\,\rho_z - \frac{1}{2}(1-2\rho)\phi_z^2\rho_z,\end{aligned} \tag{32}$$

where $E_\omega = \hbar\omega/t$, and the dimensionless speed $v\hbar/at$ has been denoted by v for simplicity. With the boundary conditions $\rho \to \rho_0$ and $\phi_z \to 0$ as $|z| \to \infty$, eq. (31) can be easily integrated to give

$$\phi_z = \frac{v(\rho-\rho_0)}{\rho(1-\rho)}. \tag{33}$$

Using this in eq. (32) and integrating, we get the following general nonlinear ordinary differential equation for ρ, valid for all values of E_e and background densities ρ_0:

$$\begin{aligned}\frac{1}{4}\rho_z^2[1-4E_e\rho(1-\rho)] \;=\; & -[(1-\rho_0)^2v^2 + \lambda_0]\rho + [2(E_e - E_\omega) - \lambda_0]\rho^2 \\ & + 2(2E_e - E_\omega)\rho^3 - 2E_e\rho^4,\end{aligned} \tag{34}$$

where λ_0 is the integration constant. It is interesting to note the natural appearance of the two energies E_ω and E_e, associated, respectively, with the frequency in the phase ϕ and the effective energy parameter in the BH model for HCB.

It is clear from eq. (34) that ρ_z^2 can be approximated by a quartic polynomial in ρ for sufficiently small values of E_e, positive or negative. (This requires V to be positive, i.e., the *nn* interaction in the BH model must be attractive.) As in the case of the GPE, we seek localized solutions for $\rho(z)$ with the asymptotic behaviour $\rho_z \to 0$ when $\rho \to \rho_0$. To this end, we write the quartic polynomial on the right-hand side of eq. (34) in the form

$$\frac{1}{4}(\rho_z)^2 = (\rho-\rho_0)^2(L\rho^2 + M\rho + N), \tag{35}$$

where L, M and N are to be found by equating the coefficients of like powers of ρ on the right-hand sides of eqs (34) and (35). Although this is straightforward, we give some details to show how the difference between the fractional- and integer-filling cases arises. We get

$$\begin{aligned} L &= -2E_e, \quad M = 2[E_e(1-\rho_0) - E_\omega), \\ N &= -2(E_e - E_\omega)\,\delta(\rho_0) - v^2, \end{aligned} \tag{36}$$

where for convenience we have used the notation $\delta(X) = 1$ for $X = 0$ and $\delta(X) = 0$ for $X \neq 0$.

We also get the consistency condition

$$(1-2\rho_0)(N+v^2) + 2(1-\rho_0)^2[E_e(1-2\rho_0) - E_\omega] = 0. \tag{37}$$

It follows at once from eqs (36) that eq. (37) is identically satisfied in the integer-filling cases $\rho_0 = 0$ and 1. In contrast, in the fractional-filling case $0 < \rho_0 < 1$ (so that N reduces to $-v^2$), eq. (37) leads to a condition on E_ω, namely,

$$E_\omega = E_e(1-2\rho_0). \tag{38}$$

Recalling from eq. (25) that $E_e(1-2\rho_0) = \hbar\omega_{\mathrm{F}}/t$, it follows that, in fractional filling, the frequency parameter ω is constrained to be equal to the fixed value ω_{F} (which depends on the effective energy of the HCB system). This is consistent with the earlier identification of the intrinsic frequency ω_{F} on general grounds, using only the asymptotic behaviour of the solution of the HGPE. In contrast, for integer filling, the frequency ω is an independently variable parameter. The constant λ_0 is also determined consistently, but we omit this because it is not relevant to the discussion in the sequel.

Turning now to eq. (35), we seek (as before) solutions of the form $\rho(z) = \rho_0 + f(z)$. Then, for all ρ_0 in the physical range [0, 1], we have

$$\left(\frac{\mathrm{d}f}{\mathrm{d}z}\right)^2 = 4f^2(Af^2 + 2Bf + D), \tag{39}$$

where

$$\left.\begin{aligned} A &= -2E_e, \\ B &= E_e(1-2\rho_0)\delta(\rho_0 - F) + (2E_e - E_\omega)\delta(\rho_0) \\ &\quad -(2E_e + E_\omega)\delta(\rho_0 - 1), \\ D &= (c^2 - v^2) = c^2\gamma^2. \end{aligned}\right\} \tag{40}$$

The quantity F in the expression for B stands for any number such that $0 < F < 1$,

$$c^2 = 2E_e\rho_0(1-\rho_0) + 2(E_\omega - E_e)\delta(\rho_0) - 2(E_\omega + E_e)\delta(\rho_0 - 1) \tag{41}$$

and

$$\gamma^2 = 1 - (v^2/c^2)\,. \tag{42}$$

Equation (39) can be solved to obtain the general functional form

$$f^{\pm}(z) = \frac{c^2\gamma^2}{\pm(B^2 + 2E_e c^2\,\gamma^2)^{1/2}\cosh(2c\gamma z) - B}\,. \tag{43}$$

We emphasize that the corresponding soliton solution $\rho(z) = \rho_0 + f(z)$ holds good when E_e is positive or negative, provided that it is sufficiently small. This solution becomes exact when $E_e = 0$, as we shall see in the next section. The solution is also valid for both fractional- and integer-filling backgrounds, although these two cases exhibit different physical characteristics. (It must also be kept in mind that E_ω is fixed as in eq. (38) in the fractional-filling case.) Owing to the particle–hole symmetry property

$$f^{\pm}(\rho_0, \omega) = -f^{\mp}(1 - \rho_0, -\omega), \tag{44}$$

it suffices to analyse solitons for the integer-filling $\rho_0 = 0$ and the fractional-filling $0 < \rho_0 \leq \frac{1}{2}$. The properties of the solitons when $\rho_0 = 1$ and $\frac{1}{2} < \rho_0 < 1$ can be read off from these results.

6. NP-type and P-type solitons

For any given ρ_0, the solutions f^+ and f^- behave differently from each other. As $\gamma \to 0$, the leading behaviour of $f^{\pm}$ is given by

$$f^{\pm}(z) \simeq \frac{c^2\gamma^2}{\pm B\big[1 + c^2\gamma^2\{(E_e/B^2) + 2z^2\}\big] - B}. \tag{45}$$

It follows that the soliton solution $f^-(z)$ vanishes at its maximum speed $v = c$. Reverting to $\rho(z) = \rho_0 + f(z)$, this leads to a density soliton which delocalizes and hence is nonpersistent at its maximum speed. Any soliton with this property will be termed an NP-type soliton.

Interestingly, at $v = c$, the solution $f^+(z)$ tends to the nonzero limit

$$f^+(z)\big|_{v=c} = \frac{B}{[E_e + 2B^2z^2]}. \tag{46}$$

Thus, the corresponding density soliton persists at its maximum speed. Any soliton with this property will be termed P-type. However, its localized profile now vanishes algebraically (rather than exponentially) as $|z| \to \infty$. In the present instance, this persistent soliton is bright for $B > 0$, and dark for $B < 0$.

Periodic soliton train

We parenthetically remark that when v exceeds c, the above P-type soliton becomes a periodic soliton train given by

$$f^+(v > c) = \frac{2(v^2 - c^2)}{[B^2 - 2E_e(v^2 - c^2)]^{1/2}\cos\big(2z\sqrt{v^2 - c^2}\big) - B}. \tag{47}$$

We shall now discuss the characteristics of various types of solitons that are supported, when the effective energy parameter E_e is zero, positive and negative.

6.1 *Effective energy parameter* $E_e = 0$

When E_e is exactly equal to zero, it is clear that there are no sound wave excitations (as the velocity of sound is proportional to $\sqrt{E_e}$). Further, the differential equation (34) for density ρ reduces to

$$\frac{1}{4}\rho_z^2 = -[(1-\rho_0)^2 v^2 + \lambda_0]\rho - (2E_\omega + \lambda_0)\rho^2 - 2E_\omega \rho^3, \tag{48}$$

with a corresponding equation for $f(z)$. The expression in eq. (43) for $f^{\pm}(z)$ then becomes an exact solution, with E_e set equal to zero in eqs (40) for the quantities A, B and D. Further, c^2 reduces to

$$c^2 = 2E_\omega\,[\delta(\rho_0) - \delta(\rho_0 - 1)]. \tag{49}$$

It is immediately clear that no solutions exist for fractional filling ($0 < \rho_0 < 1$). Hence we only need to consider integer fillings in this case.

(i) $\rho_0 = 0$

We now have $B = -E_\omega$ and $c^2 = 2E_\omega$ (so that ω must be positive). Moreover, no dark solution is possible (the density cannot fall below the zero background). The only physical solution is $f^+(z)$, which yields

$$\rho(z) = \gamma^2 \,\mathrm{sech}^2(c\gamma z). \tag{50}$$

This is an NP-type bright soliton. It is remarkable that this soliton in the strongly repulsive HCB system with a zero background density, has a sech^2 profile similar to that of the bright soliton in the weakly attractive GPE. The detailed characteristics of these two solitons are, however, quite distinct. In the latter case, the travelling waves for the density and phase must move with different speeds to support a bright soliton [24]; in contrast, in the present case they travel with the same speed. In addition, the prefactor of the sech^2 function in the latter case is not γ^2, but depends on both the speeds.

It is worth noting that bright solitons have been predicted and observed so far [2] only in weak, locally attractive systems. Our result in eq. (50) suggests that these should be looked for in strongly repulsive systems as well.

(ii) $\rho_0 = 1$

A bright soliton is not possible in this case, as the density cannot exceed unity. We now have $B = -E_\omega$ and $c^2 = -2E_\omega$ (so that ω must be negative). The solution f^+ is now ruled out (as it remains positive, causing ρ to exceed unity), while the solution f^- leads to the dark soliton

$$\rho(z) = 1 - \gamma^2 \,\mathrm{sech}^2\,(c\gamma z). \tag{51}$$

While this form of ρ is exactly the same as that of the dark soliton of the weakly repulsive GPE with background density $\rho_0 = 1$, the maximum speed of soliton in the present instance is not the speed of sound.

6.2 *Effective energy parameter* $E_e > 0$

(i) Fractional filling ($0 < \rho_0 < 1$)

This is the only case dealt with in our previous work [11–13]. We summarize the results for this case very briefly, in the interests of completeness as well as for ready comparison with the other cases to be discussed.

We have in this instance $B = E_e(1 - 2\rho_0)$ and $c^2 = 2E_e\,\rho_0(1 - \rho_0)$. At half-filling ($\rho_0 = \frac{1}{2}$), B vanishes, and the solutions $f^+(z)$ and $f^-(z)$ are mirror images of each other. Both of them lead to density solitons of the NP-type, in the sense that they delocalize as $v \to c$. On the other hand, away from half-filling, for $0 < \rho_0 < \frac{1}{2}$, we have $B > 0$, showing that $f^-(z)$ describes a NP-type dark soliton that dies as $v \to c$. In contrast, $f^+(z)$ leads to a bright soliton 'on a pedestal' for the density, that survives at $v = c$, i.e., it is a P-type soliton. Its exponentially decreasing profile alters to the algebraically decaying profile:

$$f^+(z)\big|_{v=c} = \frac{1 - 2\rho_0}{1 + 2E_e(1 - 2\rho_0)^2 z^2}. \tag{52}$$

Summarizing, for $0 < \rho_0 < \frac{1}{2}$ (respectively, $\frac{1}{2} < \rho_0 < 1$), the dark (resp., bright) soliton is of the NP-type and delocalizes fully at $v = c$, whereas the bright (resp., dark) soliton is of the P-type which survives at $v = c$, taking on an algebraic profile, and then becoming a periodic soliton train at supersonic speeds.

(ii) Integer filling, $\rho_0 = 0$

Before we discuss the details of this case, it is helpful to understand and compare the typical soliton profiles for the density ρ and the condensate density $\rho^s = \rho(1 - \rho)$ obtained from eq. (43), for two fractional-filling cases ($\rho_0 = 0.5$ and 0.25) as well as the integer-filling case $\rho_0 = 0$. In figure 1 we depict these cases for $E_e = 0.1$.

Cross-over from P-type to NP-type soliton. An interesting phenomenon occurs as we pass to the limit $\rho_0 \to 0$ of the fractional-filling case. In this limit, eq. (41) implies $c \to 0$, so that the soliton becomes static, with a fixed frequency $E_e t/\hbar$. Once this limit is reached, however, the soliton solution corresponding to the integer filling $\rho_0 = 0$ takes over, and the frequency ω becomes a freely variable parameter.

Only bright solitons can occur when $\rho_0 = 0$. From eqs (40) and (41), we find $B = (2E_e - E_\omega)$ and the maximum soliton speed $c^2 = 2(E_\omega - E_e)$. In the $\rho_0 \to 0$ limit of fractional filling, as $\hbar\omega_F/t \to E_e$ (see eq. (25)), this speed vanishes and the soliton is indeed static. But in the integer-filling case $\rho_0 = 0$ per se, ω is variable. For c to be real, we must have $E_\omega > E_e$. In addition, as we saw earlier, P-type bright solitons arise only for $B > 0$, i.e., for $2E_e \geq E_\omega$. We conclude, therefore, that when $\rho_0 = 0$, P-type bright solitons that survive at the maximum soliton speed are supported in the range of (positive) frequencies given by $2E_e > E_\omega > E_e$. However, a cross-over to the NP-type occurs at a critical frequency $E_\omega = 2E_e$. In other words, for all $E_\omega \geq 2E_e$, the solitons are NP-type bright solitons that delocalize at the maximum soliton speed. This cross-over phenomenon is illustrated in figure 2.

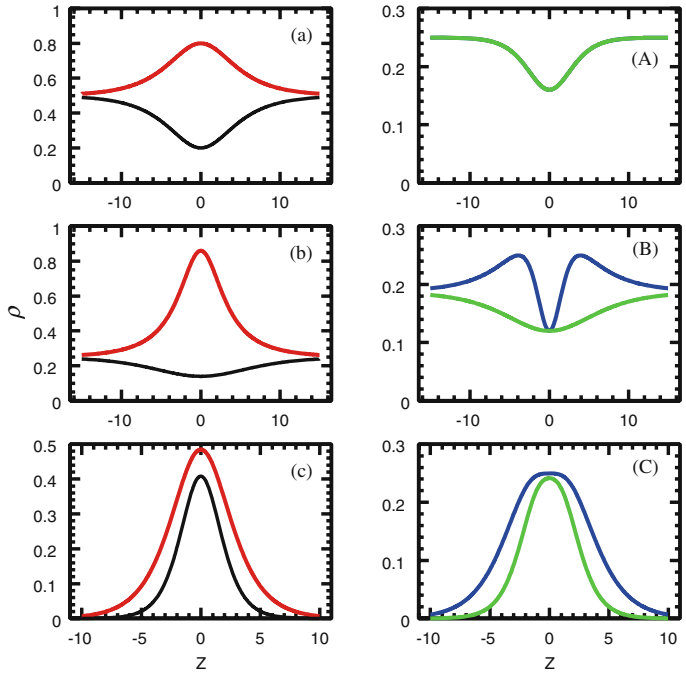

Figure 1. Solitary waves with background density (**a**) $\rho_0 = 0.5$, (**b**) $\rho_0 = 0.25$ and (**c**) $\rho_0 = 0$, for $E_e = 0.1$ and $v/c = 0.8$. The red and black lines depict the persistent (P) and nonpersistent (NP) solitons, respectively. (**A**), (**B**) and (**C**) show the corresponding condensate density $\rho^s = \rho(1-\rho)$, where the blue and green lines correspond, respectively, to P and NP solitons. When $\rho_0 = 0.5$, the plots of ρ^s for the two types coincide. When $\rho_0 = 0$, which exhibits only bright solitons, the P and NP types plotted correspond to $E_\omega = 0.15$ and 0.3, respectively.

At the critical frequency $E_\omega = 2E_e$, we have $B = 0$. Using this in eq. (43), we find the NP-type bright soliton

$$\rho(z) = \gamma\,\mathrm{sech}(2c\gamma z), \tag{53}$$

which delocalizes for $v = c = \sqrt{2E_e}$. Note that both this expression for the density, as well as that for the corresponding condensate density $\rho^s = \rho(1-\rho)$, are quite different from the form of the well-known bright soliton obtained for the GPE with an attractive interaction.

(iii) Integer filling, $\rho_0 = 1$

When $\rho_0 = 1$, only dark solitons are possible. Exploiting particle–hole symmetry, results analogous to those described above in the case $\rho_0 = 0$ can be deduced.

A final remark: Given a positive value of E_e, our analysis shows that, in the case of fractional filling, the maximum possible soliton speed corresponds to half-filling, and is given by $c = (E_e/2)^{1/2}$. In contrast, for integer filling, it appears as if the maximum

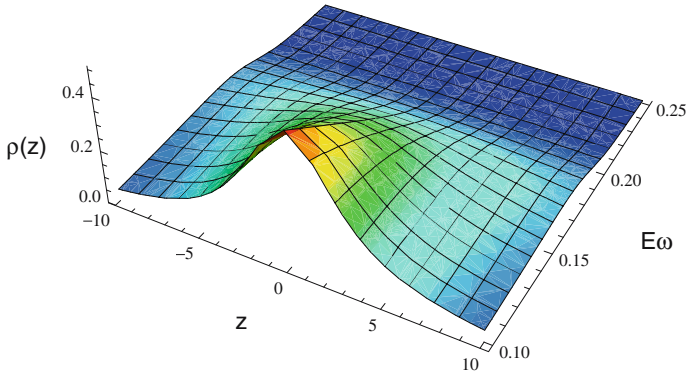

Figure 2. Solitons propagating at speed $v/c = 0.999$ for $\rho_0 = 0, E_e = 0.1$, illustrating the cross-over from P-type to NP-type with delocalization at $E_\omega > 0.2$.

speed $c = [2(E_\omega - E_e)]^{1/2}$ can keep on increasing as we increase ω. However, as shown in figure 3, the width of the soliton decreases as c increases. Hence there is an effective upper bound to the speed that is imposed by the fact that the width of the soliton cannot drop below the lattice spacing, in order for our continuum formalism to be valid.

6.3 *Effective energy parameter* $E_e < 0$

When $E_e < 0$, it is clear from eq. (41) for c^2 that the system does not support solitons for fractional filling ($0 < \rho_0 < 1$). It suffices, therefore to consider the integer-filling cases.

(i) Integer filling, $\rho_0 = 0$

It follows from eq. (41) that we must have $E_\omega > -|E_e|$ in order for c to be real. Equation (40) gives $B = -(2|E_e| + E_\omega)$. A positive value of B requires $E_\omega < -2|E_e|$, which is not consistent with a real value of c. Hence there are no soliton solutions for $B > 0$. When $B = 0$, the solution is purely imaginary, so that no solitons are possible in this case as well. Finally, for $B < 0$, it is easy to see that $f^-(z)$ is the only possible solution. This corresponds to an NP-type bright soliton solution for all $E_\omega > -|E_e|$.

(ii) Integer filling, $\rho_0 = 1$

Using the particle–hole symmetry relations, it follows from the discussion above that, in this case, an NP-type dark soliton occurs for all $E_\omega < |E_e|$.

In summary, when $E_e < 0$, no P-type soliton is possible for any value of the background density ρ_0.

This completes our discussion of soliton solutions for density ρ, and hence for the condensate density $\rho^s = \rho(1 - \rho)$. The solutions obtained for ρ in the foregoing also prove to be useful in the context of solitons in spin systems, as will be seen below.

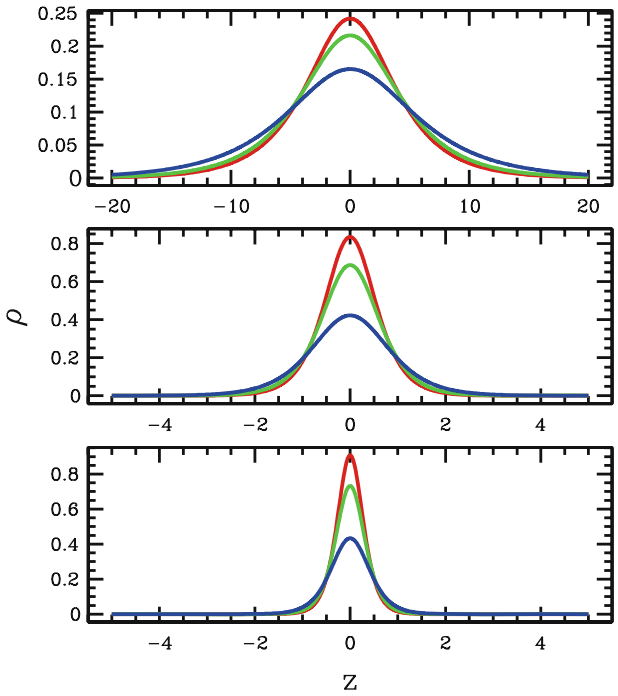

Figure 3. For $E_e = 0.05$, the three curves in each plot illustrate bright soliton profiles for $\rho_0 = 0$, for $v/c = 0.25$ (red), 0.5 (green), 0.75 (blue), respectively. The upper plot is for $c = 0.158$, which is the maximum speed of sound possible for fractional filling, attained when $\rho_0 = 0.5$. The middle and lower plots are for $c = 1$ and $c = 2$, respectively. The solitons in the middle and lower plots have speeds respectively 6.3 and 12.6 times the speeds in the upper plot. Although at $\rho_0 = 0$ the solitons have no upper limit on their speed, their profiles become extremely narrow as c becomes large.

7. HCB solitons mapped to magnetic solitons in Heisenberg spin chains

As stated in §3, the extended BH model Hamiltonian for HCB can be mapped to the quantum, spin-half, *XXZ* ferromagnetic Heisenberg Hamiltonian. Taking the expectation value of the equation of motion (16) in a spin-coherent state, we can deduce the equations of motion for the components of the spin in the corresponding classical Hamiltonian [25].

Magnetic solitons in classical Heisenberg chains have been studied for over two decades [26,27], and continue to attract attention in recent times [28]. While the order parameter for BEC is the condensate density $\rho^s = \rho(1-\rho)$, the relevant order parameter for the spin system is S^z, which can be found from the HCB boson density ρ on using the identification

$$S^z = \frac{1}{2} - \rho. \tag{54}$$

Thus, all the soliton solutions for $\rho(z)$ which we have found in the foregoing will also yield the corresponding magnetic soliton solutions for $S^z(z)$. The mapping between

the BEC and the magnetic systems also helps to provide some insights into the results obtained in the former case.

The analysis described in the preceding sections shows that, in all instances, the phase $\phi(x,\tau)$ must be of the form $\omega\tau+\phi(x-v\tau)$ (recall eq. (3)), i.e., the additive, purely time-dependent term $\omega\tau$ is necessary to obtain soliton solutions. In the context of a spin system, ω is just the spin precession frequency in the presence of an external magnetic field along the z-axis. An appropriate field term must therefore be present in the effective Hamiltonian of the spin system. Thus, the gauge-transformed evolution equation (23), which led ultimately to the soliton solutions in eq. (43), also describes the solitons in the continuum dynamics of the following dimensionless anisotropic Heisenberg spin Hamiltonian:

$$H_{\text{eff}}/t = -\sum_{\langle j,l\rangle}\mathbf{S}_j\cdot\mathbf{S}_l + E_e\sum_{\langle j,l\rangle}S_j^zS_l^z - E_\omega\sum_j S_j^z, \tag{55}$$

where E_e and E_ω now represent, respectively, the anisotropy energy and the magnetic field along the z-axis that causes the desired spin precession. As in the BEC problem, three cases arise, corresponding, respectively, to positive, zero and negative values of E_e. These will be considered in turn. Corresponding to the background density ρ_0 in the BEC case, the background value of the order parameter in the spin system is

$$\bar{S}^z = \frac{1}{2}-\rho_0. \tag{56}$$

The order parameter $S^z(z)\to\bar{S}^z$ asymptotically. The range $0\le\rho_0\le 1$ translates to $\frac{1}{2}\ge\bar{S}^z\ge-\frac{1}{2}$. Integer and fractional fillings correspond, respectively, to $\bar{S}^z=\pm\frac{1}{2}$ and $-\frac{1}{2}<\bar{S}^z<\frac{1}{2}$. In particular, half-filling ($\rho_0=\frac{1}{2}$) corresponds to $\bar{S}^z=0$.

(a) $E_e>0$

In physical terms, this case corresponds to an easy-plane anisotropic spin chain. Once again, two subcases must be distinguished.

(i) $-\frac{1}{2}<\bar{S}^z<\frac{1}{2}$: As we have already seen in the BEC system, in this case the frequency ω is fixed at the value ω_{F} given by $\hbar\omega_{\text{F}}/t = 2E_e\bar{S}^z$. The effective Hamiltonian in eq. (55) becomes

$$H_{\text{eff}}/t = -\sum_{\langle j,l\rangle}\mathbf{S}_j\cdot\mathbf{S}_l + E_e\sum_{\langle j,l\rangle}S_j^zS_l^z - 2E_e\bar{S}^z\sum_j S_j^z. \tag{57}$$

Unlike the case of usual spin chains, the 'external' field is not an independent quantity, but depends on the anisotropy E_e and $\bar{S}^z$. There are two competing terms in H_{eff}: the easy-plane anisotropy tends to make spins lie in the xy-plane, but the magnetic field tends to align spins along the z-axis. (This field encodes the particle–hole imbalance $(1-2\rho_0)$ in the background.) At half-filling, the magnetic field vanishes. Hence neither the positive nor the negative z-direction is preferred to the other, and the excitations are symmetric about the easy plane. This helps us to understand why the solitons in figure 1a are mirror images of each other.

Away from half-filling, the magnetic field is nonzero, and this symmetry is lost (see figure 1b). In general, both NP- and P-type magnetic solitons occur. The solitons we

obtain for spin-1/2 are similar to the A- and B-type rotary wave solutions [27] found for magnetic solitons in spin S, easy-plane chains with a specific type of external field which depends on the anisotropy and the boundary condition on S^z. It is interesting that this type of spin Hamiltonian appears in a natural fashion in the extended BH model for HCB. (ii) $\bar{S}^z = \pm 1/2$: In this case the precession frequency ω, which is necessary to create a soliton, is no longer fixed. The field term in the spin Hamiltonian in eq. (55) is proportional to ω. Translating our results for the limit $\rho_0 \to 0$ discussed earlier, we have P-type magnetic solitons that persist even at their maximum speed (which depends on ω) for a range of fields E_ω, beyond which they cross over to NP-type magnetic solitons.

(b) $E_e = 0$ and (c) $E_e < 0$

These cases represent, respectively, the isotropic and easy-axis anisotropic spin chains. It is clear that $\bar{S}^z$ can only be $\pm 1/2$ in these cases. Hence, ω is a variable parameter. However, in contrast to the case of the easy-plane spin chain, these systems support only NP-type solitons for all ω.

We remark that in the existing literature [26,27], magnetic soliton solutions for S^z in the classical isotropic chain ($E_e = 0$) as well as the easy-plane ($E_e > 0$) and easy-axis ($E_e < 0$) anisotropic chains have been treated individually, on a case-by-case basis. In contrast, the derivation we have presented permits us to find soliton solutions in all the cases in a unified manner. Equation (43) provides a single expression from which the functional forms of the solitons and their characteristics can readily be deduced in all the cases of interest.

8. Summary and discussion

We have provided a unified formulation for finding solitary waves for all background densities, in the BEC of strongly repulsive bosons, described by a hard-core boson (HCB) system. Using an extended Bose–Hubbard model for HCB, which also includes nearest-neighbour attractive interactions on the lattice, we show that in the continuum version, the condensate order parameter of this system satisfies eq. (19), which we have named the HGPE. Our comprehensive analysis also includes the GPE for weakly repulsive BEC, arising from the BH model of normal bosons. Interestingly, the GPE also emerges on neglecting certain nonlinear terms in the HGPE for low densities.

We find that, while the infinite on-site repulsion condition $U/t \to \infty$, for HCB in the BH model completely delocalizes the dark soliton in the GPE (see eq. (14)), the addition of a finite nn attractive potential $V \sim t\ (\ll U)$ is sufficient to localize the dark soliton and even (in some cases) support bright solitons. As our results derived from eq. (43) for the HGPE show, the behaviour of the soliton depends on the value of the condensate background density and on the sign and magnitude of the effective energy parameter E_e.

The methodology we have developed for finding soliton solutions of both the GPE and the HGPE with various background densities in BEC provides an integrated framework that also proves useful in understanding these nonlinear modes in magnetic spin chains. Further, it brings out certain universal aspects of the solutions, as well as certain distinguishing features. By enabling an integrated treatment of the GPE and of the HGPE

for various background densities (leading to eqs (8) and (35), respectively), our analysis brings out a kind of universality in the description of solitary waves whose amplitude and width are expressed in terms of the maximum speed c and the corresponding contraction factor γ (compare the solutions given by eqs (14) and (43)).

We now summarize our results for solitons in the HGPE. Solitons in the presence of a background condensate density (i.e., when $0 < \rho_0 < 1$) and in its absence (i.e., when $\rho_0 = 0$ or 1) encode a fundamental distinction. Although two competing energy scales E_e and E_ω appear in general in the HCB system, our systematic analysis shows that in the former case these get related, leading to a fixed frequency, whereas in the latter case they remain independent parameters.

When the background condensate density is nonzero, solitons exist only for $E_e > 0$, with the speed of sound as the maximum speed of the soliton. The soliton is characterized by its speed v alone, while its associated frequency $\omega_{\rm F}$ is a constant, fixed by the background ρ_0 and the system parameters. For this case, the two species of condensate density solitons coexist: an NP-type dark soliton and a novel P-type bright soliton which persists even at the speed of sound.

When the background condensate density vanishes, solitons exist for $E_e > 0$ as well as for $E_e \leq 0$. There is neither intrinsic speed of sound, nor a fixed frequency. The soliton solution is a function of both its speed v and its variable frequency ω. Further, the maximum speed c of the soliton depends upon ω. The cases $E_e > 0$ and $E_e \leq 0$ are distinct from each other, the behaviour in the former instance being somewhat more intricate.

When $E_e > 0$ (and the background condensate density is zero), the two species (the P-type and the NP-type) of solitons do not coexist. The frequency parameter ω provides an additional independent energy scale E_ω in this case. Considering, for example, the case $\rho_0 = 0$, the P-type bright solitons (in the density ρ) that survive even at the maximum speed $v = c$ only exist if $E_e < E_\omega < 2E_e$. This shows that the energy E_ω associated with the background should be at least E_e, to create even a static soliton excitation that rises above the background. Energies higher than this make the soliton move, with the amplitude remaining finite even at its maximum (ω-dependent) speed $v = c$. This shows its persistent nature. However, the amplitude of the soliton at $v = c$ steadily decreases as a function of ω, till it vanishes at a critical frequency given by the condition $E_\omega = 2E_e$, signalling a cross-over to an NP-type soliton for $E_\omega > 2E_e$. This phenomenon is illustrated in figure 2.

On the other hand, when $E_e \leq 0$ (and the background condensate density is zero), only one species of soliton can occur, namely, the NP-type bright soliton for the condensate density.

A novel aspect of solitons in the HCB system described by the HGPE is the possibility of creating very high-speed localized modes in a system whose background has vanishing condensate density, by increasing the soliton frequency ω. The zero-background solitons for this strongly repulsive system can indeed be made to propagate with speeds that are much higher than the maximum speed possible (attained at half-filling, $\rho_0 = 1/2$) when the solitons move in a background with a nonvanishing condensate density. This is illustrated in figure 3 for $E_e > 0$, but it remains true even when $E_e < 0$.

The 'Soliton Tree' diagram in figure 4 summarizes various possible solitary wave solutions for the density in the HCB system, providing a comprehensive picture of its nonlinear modes.

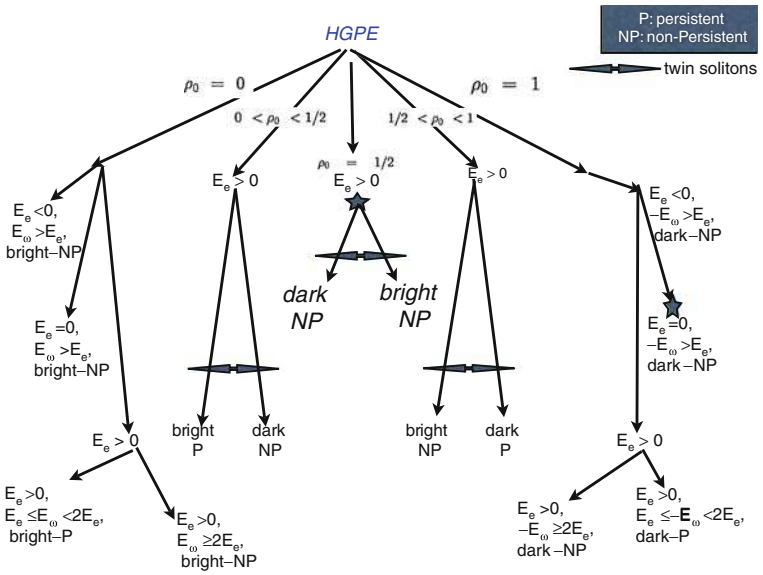

Figure 4. Soliton Tree: Classification of different types of density solitons in the HCB system considered. The star indicates that the corresponding soliton has a form similar to that of the GPE.

Finally, we have shown that, by using the relationship $\rho = \frac{1}{2} - S^z$ between the density in the HCB system and the order parameter in the spin system, the entire analysis can be carried over to find and describe magnetic solitons in isotropic and anisotropic ferromagnetic spin chains in the presence of a magnetic field, in a consolidated fashion.

Soliton propagation has been studied experimentally in BEC using various techniques [6] such as the phase-imprinting method [1–3], which manipulates the initial BEC phase without affecting its density, the density-engineering method [4,5] which creates an appropriate initial form for the density without affecting the BEC phase and the quantum-state engineering method [3,5] which manipulates both the density and the phase. Suggestions for experimental realizations of the HCB system have been discussed in detail in [18]. We hope that our detailed theoretical results and predictions will motivate experimental research on BEC solitons in the strongly interacting HCB system we have studied.

Acknowledgements

RB thanks the Department of Science and Technology, India, for financial support.

References

[1] S Burger *et al*, *Phys. Rev. Lett.* **83**, 5198 (1999)
J Denschlag *et al*, *Science* **287**, 97 (2000)
[2] K Strecker *et al*, *Nature* **417**, 150 (2002)
[3] C Becker *et al*, *Nature Phys.* **4**, 496 (2008)
S Stellmer *et al*, *Phys. Rev. Lett.* **101**, 120406 (2008)

[4] C Dutton *et al*, *Science* **293**, 663 (2001)
J J Chang, P Engels and M A Hoefer, *Phys. Rev. Lett.* **101**, 170404 (2008)
[5] S Burger *et al*, *Phys. Rev. A* **65**, 043611 (2002)
[6] D J Frantzskakis, *J. Phys. A: Math. Theor.* **43**, 213001 (2010)
[7] Although solitons are, strictly speaking, solitary waves that retain their characteristics intact even after collisions with each other, in this paper we use the term 'soliton' to denote any solitary wave.
[8] C J Pethick and H Smith, *Bose–Einstein condensation in dilute gases* (Cambridge University Press, Cambridge, 2001)
[9] See, for instance, L Pitaevskii and S Stringari, *Bose–Einstein condensation* (Oxford University Press, Oxford, 2003)
[10] See, for example, T Dauxois and M Peyrard, *Physics of solitons* (Cambridge University Press, Cambridge, 2006) and references therein
[11] R Balakrishnan, I I Satija and C W Clark, *Phys. Rev. Lett.* **103**, 230403 (2009)
[12] R Balakrishnan and I I Satija, *Pramana – J. Phys.* **77**, 929 (2011)
[13] I I Satija and R Balakrishnan, *Phys. Lett. A* **375**, 517 (2011)
[14] See, for example, S Sachdev, *Quantum phase transitions* (Cambridge University Press, Cambridge, 1999)
[15] T Matsubara and H Matsuda, *Prog. Theor. Phys.* **16**, 569 (1956)
[16] J M Radcliffe, *J. Phys. A* **4**, 313 (1971)
[17] W Reinhardt, I I Satija, B Robbins and C W Clark, arXiv:quant-phys1102.4042
[18] C P Rubbo, I I Satija, W P Reinhardt, R Balakrishnan, A M Rey and S R Manmana, *Phys. Rev. A* **85**, 053617 (2012)
[19] J H Denschlag *et al*, *J. Phys. B* **35**, 3095 (2002)
S Peil *et al*, *Phys. Rev. A* **67**, 051603 (2003)
[20] J S Langer, *Phys. Rev.* **167**, 183 (1968)
[21] A D Jackson, G M Kavoulakis and C J Pethick, *Phys. Rev. A* **58**, 2417 (1998)
[22] L Salasnich, A Parola and L Reatto, *Phys. Rev. A* **65**, 043614 (2002); *ibid.* **69**, 045601 (2004)
[23] U Roy, B Shah, K Abhinav and P K Panigrahi, *J. Phys. B* **44**, 035302 (2011)
[24] A C Scott, F Y F Chu and D W McLaughlin, *Proc. IEEE* **61**, 1443 (1973)
[25] R Balakrishnan and A R Bishop, *Phys. Rev. Lett.* **55**, 537 (1985). These equations of motion can be obtained for general S, but we are only concerned with the spin-$1/2$ case here
[26] H J Mikeska and M Steiner, *Adv. Phys.* **40**, 191 (1990)
[27] A M Kosevich, B A Ivanov and A S Kovalev, *Phys. Rep.* **194**, 117 (1990)
[28] J Lu *et al*, *Phys. Rev. E* **79**, 016606 (2009)
M A Hoefer, T J Silva and M W Keller, *Phys. Rev. B* **82**, 054432 (2010)